

Quasielastic neutron scattering study of the methyl group dynamics in polyisoprene

R. Zorn^{a)}

Institut für Festkörperforschung, Forschungszentrum Jülich, D-52425 Jülich, Germany

B. Frick

Institut Laue-Langevin, BP 156, F-38042 Grenoble Cedex 9, France

L. J. Fetters

Exxon Research and Engineering, Annandale, New Jersey 08801

(Received 24 July 2001; accepted 11 October 2001)

In this paper the microscopic dynamics of methyl side groups in polyisoprene is studied by means of inelastic neutron scattering. By combining time-of-flight and backscattering technique a range of four decades can be obtained (0.2 ps–2 ns). The two experimental results were combined in the time domain by using an inverse Fourier transform. Multiple scattering effects were treated by a novel procedure acting on the time-dependent intermediate scattering function $S(Q, t)$. In the description of the data incoherent and coherent scattering from “fixed” atoms was taken into account, i.e., atoms in the main chain that move too slow to be observed in the dynamical window of the experiment. In this way good agreement with the rotation rate distribution model of a threefold jump could be obtained. Seeming discrepancies of the elastic incoherent structure factor vanish after the corrections mentioned above. The distribution of activation energies can be expressed as a Gaussian with an average of 9.7 kJ/mol and a width of 30%. It turns out that the width calculated by the model fit of the data depends on the use of the multiple scattering correction while the average activation energy can also be obtained reliably without that correction from high Q spectra. © 2002 American Institute of Physics. [DOI: 10.1063/1.1424319]

I. INTRODUCTION

The motion of methyl side groups in polymers has been a topic of considerable interest during the last decades. A reason for this interest arising from application objectives is the study of the relaxation mechanisms of polymer side groups that lead to energy dissipation at temperatures below the glass transition improving the mechanical properties of such polymers.¹ Among the possible side groups, the methyl group is the most simple, with only one rotational degree of freedom and therefore a good model to start with. Furthermore, its motion is fast if compared to larger side groups and therefore easier to observe by inelastic and quasielastic neutron scattering.

Another more fundamental motivation is the interest in energy landscapes² in glass-forming polymers. The total energy landscape in the configurational space is clearly too complex to be accessed completely in an experiment. But the distribution of torsional potentials probed by the methyl group in different surroundings caused by the amorphous structure may give a representative simplified picture. The results can also be used to check the accuracy of computer simulations³ of such amorphous polymers.

Finally, interest has grown in the quantum mechanical properties of the methyl group. Because of its low moment of inertia a tunnel effect at low temperatures is expected, as it was observed before in low molecular crystalline materi-

als. Its apparent absence could be recently explained as a direct consequence of the distribution of torsional potentials.⁴

Neutron scattering investigations of the (nonquantum) dynamics of the methyl group dynamics in polymers can be divided into two classes: (1) Inelastic neutron scattering to observe the libration motion.^{5,6} This technique gives information about the torsional potential near its minima. (2) Quasielastic neutron scattering (QENS) to observe the thermally activated hopping over the energy barriers.^{5–9} The latter probes the barrier height of the potential.

A special advantage of neutron scattering in these investigations is the high incoherent scattering cross section of protons (80.3 barn) compared to the total scattering cross sections of deuterium (7.6 barn) and carbon nuclei (5.6 barn). By selectively replacing hydrogen atoms in the polymer main chain by deuterium, their scattering can be suppressed. In this way the relative scattering contribution of the (23%) methyl group hydrogen atoms in polyisoprene can be enhanced to up to about 70% of the total scattering.

The first QENS experiments were interpreted with only a single barrier height.⁵ It became clear that this was an oversimplification from which unphysical results emerged. In consequence, distributions were assumed either implicitly by using a nonexponential relaxation function (namely the Kohlrausch function⁸) or explicitly assuming a distribution of relaxation times.^{6,7} In this paper we will follow the second route because a distribution of relaxation times can directly be related to a distribution of energy barriers. The relaxation

^{a)}Corresponding author. Electronic mail: r.zorn@fz-juelich.de

time distributions corresponding to nonexponential relaxation functions are also often unknown and the shape of the nonexponential function is expected to change with temperature. There is also empirical evidence that the assumption of the symmetrical lognormal distribution of relaxation times fits the data better than the asymmetric one implied by the Kohlrausch law.⁹

II. EXPERIMENTAL DETAILS

A. Material

In order to obtain predominant incoherent scattering from the methyl groups the experiment was done on chain deuterated polyisoprene-d5 (PI-d5). The sample used here was the same already used in an earlier experiment.⁶ It was prepared by anionic polymerization with a molecular weight $M_w = 1.1 \times 10^5$ and a polydispersity of less than 1.06. The microstructural composition was about 93% 1,4- and 7% 3,4-polyisoprene. Undeuterated PI of the same molecular weight and microstructure has a glass temperature $T_g = 207$ K.¹⁰ Full deuteration leads to an increase of T_g of about 3 K (estimated from DSC measurements on polybutadiene¹¹ and deuterated polybutadiene¹²), so that for the partially deuterated compound, $T_g \approx 209$ K can be estimated.

¹H NMR measurements showed that the deuteration of the main chain was only $90.8 \pm 0.3\%$. Because of the high incoherent scattering cross section of protons, this has a strong consequence on the composition of the neutron scattering signal. While in the earlier study⁶ it was assumed that 77% of the total scattering was incoherent from the methyl groups, we now have to accept a lower value of 69%.

B. Methods

In this study two inelastic neutron scattering instruments at the Institut Laue Langevin (Grenoble, France) were used: The time-of-flight spectrometer IN5 for moderate energy resolution and the backscattering spectrometer IN16 for high resolution.

1. IN5

The time-of-flight chopper spectrometer IN5 was used with an incident wavelength $\lambda_i = 6.75$ Å, resulting in a wave vector range $Q = 0.4$ – 1.7 Å⁻¹ for elastic scattering. Due to the kinematic restriction only energies up to 1.4 meV for the lowest Q and 10.3 meV for the highest Q could be accessed. The energy resolution width was about 40 μeV (full width at half-maximum, FWHM) slightly broadening toward high Q . The sample was (as in the case of the IN16 experiment) a foil with 0.15 mm thickness curled on a cylinder of 22 mm diam. The calculated scattering efficiency of this sample shape is 13% and it is expected that the cylindrical geometry leads to an isotropic distribution of multiple scattering. Figure 1 shows representative data from IN5 interpolated to constant wave vector Q .

2. IN16

The backscattering spectrometer IN16 was used in the standard setup with unpolished Si (111) monochromator/

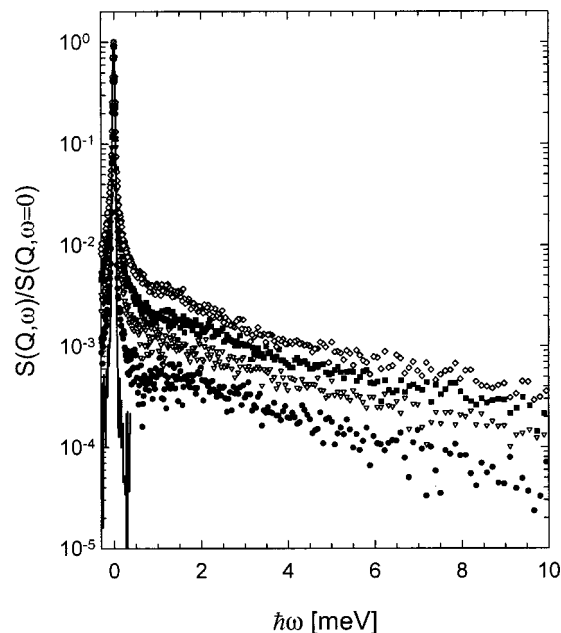


FIG. 1. Neutron time-of-flight spectra $S(Q, \omega)$ of PI-d5 obtained on IN5 normalized to their elastic peak maxima. Spectra from different detectors are interpolated to constant $Q = 1.57$ Å⁻¹. Temperatures: 90 K (circles), 150 K (triangles), 200 K (squares), 240 K (diamonds), and resolution ≈ 2 K (line).

analyzer. This corresponds to a wavelength of 6.271 Å and an energy resolution of 1 μeV (full width at half-maximum, FWHM). The energy range available by Doppler shift was ± 14 μeV. The detector signals were grouped into five groups between $Q = 0.43$ and 1.57 Å⁻¹ in order to obtain sufficient statistics. Each of these detector groups have a width of 20°, which corresponds to $\Delta Q = 0.22$ Å⁻¹ at low Q and $\Delta Q = 0.11$ Å⁻¹ at high Q . Figure 2 shows spectra from the highest Q detector group.

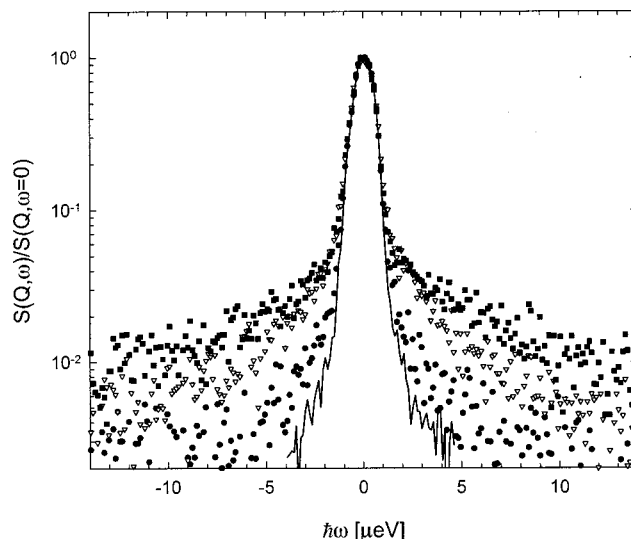


FIG. 2. Neutron backscattering spectra $S(Q, \omega)$ of PI-d5 obtained on IN16 normalized to their elastic peak maxima. Three detectors with wave vectors $Q = 1.49$ – 1.64 Å⁻¹ have been averaged. Temperatures: 90 K (circles), 130 K (triangles), 170 K (squares), and resolution ≈ 2 K (line).

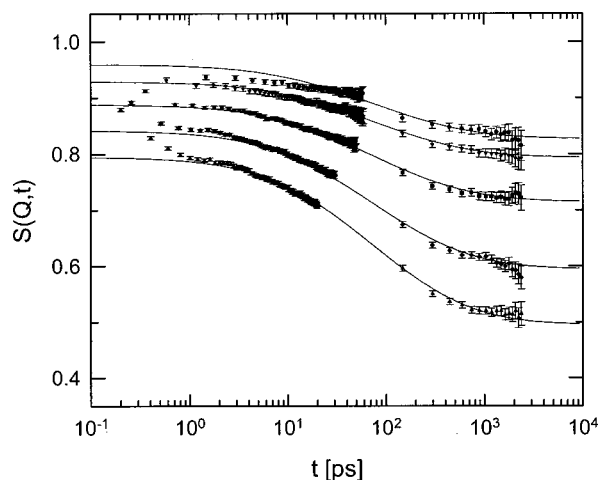


FIG. 3. Intermediate scattering function $S(Q,t)$ (before a multiple scattering correction) of PI-d5 at $T=170$ K for different wave vectors Q : $Q=0.43 \text{ \AA}^{-1}$ (circles), $Q=0.76 \text{ \AA}^{-1}$ (triangles down), $Q=1.06 \text{ \AA}^{-1}$ (squares), $Q=1.33 \text{ \AA}^{-1}$ (diamonds), and $Q=1.57 \text{ \AA}^{-1}$ (triangles up). The points with $t < 60$ ps originate from the Fourier transform of IN5 data; those with $t \geq 150$ ps from IN16 data. The lines are fits with the model described in Sec. IV.

C. Time domain analysis

In order to combine neutron scattering data from IN5 and IN16, the scattering functions were Fourier transformed by numerical calculation of the intermediate scattering function,

$$S(Q,t) = \int_{-\infty}^{+\infty} S(Q,\omega) \exp(i\omega t) d\omega. \quad (1)$$

By Fourier transform to the time domain, the convolution with the resolution function implied in the measuring process is converted into a product and the intermediate scattering function corrected for the resolution effect can be obtained as the ratio¹³

$$S(Q,t) = \frac{\tilde{S}(Q,t)}{R(Q,t)}, \quad (2)$$

where $\tilde{S}(Q,t)$ is obtained directly from the measured data. For the resolution function $R(Q,t)$, the spectrum of the sample at $T=2$ K has been used. Figure 3 shows the intermediate scattering functions $S(Q,t)$ at several Q values resulting without a multiple scattering correction. Even without regard to the attempted fit indicated in this figure, it is clear that the data do not match for low Q and do not extrapolate to 1 for $Q \rightarrow 0$. This is a clear consequence of multiple scattering that enhances the inelastic part for small angles, which means a reduction of $S(Q,t)$.

Figure 4 shows $S(Q,t)$ after the multiple scattering correction described in the Appendix. The multiple scattering correction parameter for IN5 was determined to $s=0.19$ by imposing the asymptotic behavior $S(Q,t) = 1 - aQ^2 + O(Q^4)$. For IN16 this was not possible because the low Q detectors did not allow a reliable extrapolation $Q \rightarrow 0$. Therefore, for IN16 $s=0.25$ was determined by optimizing the continuity to the IN5 data. The slightly higher value for the backscattering

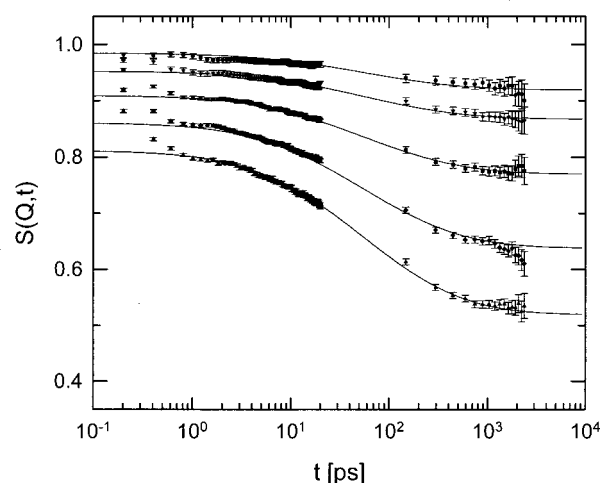


FIG. 4. Intermediate scattering function $S(Q,t)$ (after multiple scattering correction) of PI-d5 at $T=170$ K for different wave vectors Q : $Q=0.43 \text{ \AA}^{-1}$ (circles), $Q=0.76 \text{ \AA}^{-1}$ (triangles down), $Q=1.06 \text{ \AA}^{-1}$ (squares), $Q=1.33 \text{ \AA}^{-1}$ (diamonds), and $Q=1.57 \text{ \AA}^{-1}$ (triangles up). The points with $t < 60$ ps originate from the Fourier transform of IN5 data; those with $t \geq 150$ ps from IN16 data. The lines are fits with the model described in Sec. IV.

instrument is expected because a part of the neutron beam passes the sample a second time after reflection by the analyzer.

It may be observed that the $S(Q,t)$ raw values from IN5 have different t ranges and spacing while the corrected values do not. The reason for this is that the IN5 resolution is better for low Q , but the energy range is smaller due to the kinematic restriction. In order to apply the multiple scattering correction in the time domain, all $S(Q,t)$ sets had to be interpolated to the same set of t values. In this process the IN5 values for $t > 20$ ps that are present in the original $S(Q,t)$ for $Q \leq 1.33 \text{ \AA}^{-1}$ are lost.

III. ELASTIC INCOHERENT STRUCTURE FACTOR (EISF)

The motion of the methyl group protons that is predominantly observed in this experiment is a superposition of various processes: thermal vibrations, “fast process,”¹⁴ methyl group reorientation, and α relaxation. Thermal vibrations and a “fast process” are restricted to the short time range $t \leq 1$ ps. They can be seen as an initial decay of $S(Q,t)$ in Figs. 3 and 4. Because all experiments were done at temperatures below the glass transition, the α relaxation is too slow to be visible in the time range below 2 ns examined here.

The dynamics in the time window 2 ps–2 ns can be described by comprising the faster processes into a Debye–Waller factor (DWF) $\exp(-\langle u_{\text{fast}}^2 \rangle Q^2/3)$ and those that are effectively “frozen” on that time scale into an elastic incoherent structure factor (EISF) $A(Q)$, yielding

$$S_{\text{methyl}}(Q,t) = e^{-\langle u_{\text{fast}}^2 \rangle Q^2/3} \{ [1 - A(Q)] \phi(t) + A(Q) \}. \quad (3)$$

It can be seen easily from this expression that the EISF is the ratio $S_{\text{methyl}}(Q, t \rightarrow \infty) / S_{\text{methyl}}(Q, t \rightarrow 0)$.

Here $\phi(t)$ describes the dynamics of the methyl group reorientation while $A(Q)$ describes its spatial pattern (e.g.,

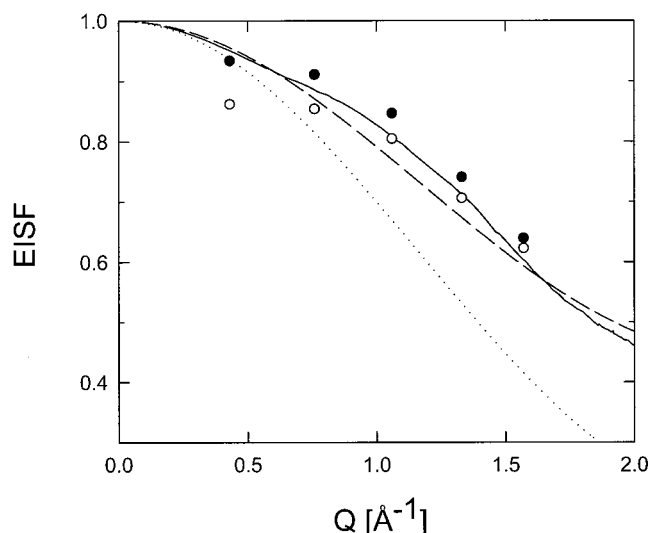


FIG. 5. An elastic incoherent structure factor from uncorrected $S(Q, t)$ values (empty symbols) and multiple-scattering corrected $S(Q, t)$ values (filled symbols). The lines represent the expectation from the threefold jump rotation model with different fractions of the scattering due to “fixed” atoms: $c_{\text{fix}}=0$ (dotted), $c_{\text{fix}}=0.305$ (dashed), $c_{\text{fix}}(Q)$, as described in the text (continuous).

jump or diffusion). The former has been adopted from the rotation rate distribution model (RRDM)^{7,9} as a superposition of single processes with different relaxation times:

$$\phi(t) = \int_{\tau=0}^{\infty} \exp(-t/\tau) g(\ln \tau) d \ln \tau, \quad (4)$$

where the distribution of the relaxation times is lognormal:

$$g(\ln \tau) = \frac{1}{\sqrt{2\pi}\sigma_{\ln \tau}} \exp\left(-\frac{(\ln \tau - \ln \tau_0)^2}{2\sigma_{\ln \tau}^2}\right). \quad (5)$$

It has to be conceded that the choice of the function $\phi(t)$ may have some influence on the EISF values calculated here. But for the temperature 170 K chosen here, the relaxation lies well within the experimental window. So the fit of expression (3) does not involve much of an extrapolation and the ratio $S_{\text{fit}}(Q, t \rightarrow \infty)/S_{\text{methyl}}(Q, t \rightarrow 0)$ is already well defined by the data itself.

The most straightforward assumption for the EISF is that of a threefold jump rotation because of the three equivalent energy minima with respect to the rotation angle of the methyl group:

$$A_{3\text{-jump}}(Q) = \frac{1}{3} \left(1 + 2 \frac{\sin(\sqrt{3}QR)}{\sqrt{3}QR} \right), \quad (6)$$

where $R=1.027 \text{ \AA}$ is the radius of the circle spanned by the positions of the hydrogen nuclei.

Figure 5 shows the EISF calculated from (6) together with the values obtained experimentally fitting (3) to the uncorrected and the multiple-scattering corrected $S(Q, t)$. It can be seen that the multiple-scattering correction removes the fundamental problem that $A(Q)$ does not extrapolate to one for $Q \rightarrow 0$ but otherwise does not much improve the

agreement. In the following we show that the remaining deviations can be explained to a large extent by several corrections.

The most evident one is the correction due to scattering from the polymer chain itself, which is essentially elastic at the temperatures here ($T < T_g$). This correction has already been derived earlier and gives rise to an apparent EISF that is higher:⁶

$$A_{\text{app}}(Q) = (1 - c_{\text{fix}})A(Q) + c_{\text{fix}}. \quad (7)$$

Here c_{fix} denotes the fraction of the neutron scattering cross section due to atoms fixed in the polymer chain. It is justified to treat their scattering as elastic because all experiments were done at sufficiently low temperatures where the time scale associated to the glass transition is much longer than that of the methyl group motion. The originally used value⁶ $c_{\text{fix}}=0.234$ from the ideal isotopical composition has to be increased to $c_{\text{fix}}=0.305$ because of the incomplete deuteration detected by our NMR measurement. Although the agreement is now much improved, the Q dependence of $A(Q)$ is still not in complete agreement with the experimental values.

One of the reasons for the remaining deviation is that Eq. (7) does not take into account that a significant part of the scattering from the “fixed” atoms is coherent and therefore has a Q dependence. This can be taken into account by introducing a Q -dependent correction factor:

$$c_{\text{fix}}(Q) = \frac{\frac{d\sigma_{\text{coh}}}{d\Omega}(Q) + \frac{\sigma_{\text{inc}}^{\text{chain H}}}{4\pi}}{\frac{d\sigma_{\text{coh}}}{d\Omega}(Q) + \frac{\sigma_{\text{inc}}^{\text{chain H}}}{4\pi} + \frac{\sigma_{\text{inc}}^{\text{methyl H}}}{4\pi}}. \quad (8)$$

In deriving this expression it has been taken into account that carbon nuclei have virtually no incoherent cross section. The coherent scattering from the methyl group hydrogen nuclei was considered as if it were from fixed atoms. This is justified if their motion is a reorientation between indistinguishable positions. Nevertheless, if this would not be true the induced error would not be large because it only accounts for 2% of the total scattering. It can be seen that the correction reduces to the previous at the Q values where the coherent differential scattering cross section is equal to its high Q limit $\sigma_{\text{coh}}/4\pi$.

It is clear that this correction requires knowledge of the coherent differential scattering cross section $d\sigma_{\text{coh}}/d\Omega$ on an absolute scale. This information can only be obtained by use of polarization analysis.^{15,16} For this purpose we used the data of Ref. 17 after multiple scattering correction by a procedure described elsewhere,¹⁸ similar to that of Ref. 19.

The continuous line in Fig. 5 shows the calculated EISF including this final correction. It can be seen that the trend of the correction is correct reducing the deviation in the range of strong coherent scattering. Nevertheless, there is a remaining difference that can be attributed to several uncertainties: (i) As explained in Sec. II C there is some uncertainty remaining in the determination of the multiple scattering parameter s that crucially influences the EISF. (ii) In order to avoid inelasticity effects, the diffraction experiment of Ref. 17 has been done at low temperature ($T \approx 4 \text{ K}$). Although

changes in the coherent scattering from polymers are usually small even over large temperature ranges,²⁰ certain differences are to be expected. (iii) Similar to the multiple scattering correction of the $S(Q,t)$ data, also that of the diffraction data involves a parameter expressing the strength of the multiple scattering. The determination of this parameter requires exact knowledge of the transmission that was not available here. Taking into account these uncertainties, the remaining deviation of the EISF may be insignificant.

It is important to note that these results are *compatible* with the threefold jump rotation model, but do not *prove* its validity. This is because in the low Q range investigated here, Eq. (6) is not much different from its low Q expansion, $1 - \frac{1}{3}Q^2R^2$. Therefore all models whose EISF have this asymptotic behavior (e.g., the rotational diffusion model) are equally possible.

IV. DYNAMICS

While the preceding section was mainly concerned with the structural aspects of the methyl group motion reflected in the EISF, we will now deal with the dynamics and its temperature dependence. In the context of the last section the function $\phi(t)$ describing the relaxation was only a fit function enabling the determination of $S_{\text{methyl}}(Q, t \rightarrow \infty)$ and $S_{\text{fit}}(Q, t \rightarrow 0)$. One could also use—as in Ref. 8—a Kohlrausch function $\phi(t) = \exp[-(t/\tau)^\beta]$ without major changes to the results. In this section instead we will assign a microscopic interpretation⁷ to the specific form of $\phi(t)$ chosen in Eq. (4).

As a first hypothesis we assume that the reorientation of the methyl groups is an activated process involving a distribution of activation energies $G(E_A)$ and the attempt frequency τ_∞^{-1} is the same for all methyl groups. Then a distribution of relaxation times,

$$g(\ln \tau) = k_B T G[k_B T \ln(\tau/\tau_\infty)], \quad (9)$$

results from the Arrhenius relation $\tau = \tau_\infty \exp(E_A/k_B T)$. Especially, if a normal distribution,

$$G(E_A) = \frac{1}{\sqrt{2\pi}\sigma_{E_A}} \exp\left(-\frac{(E_A - E_0)^2}{2\sigma_{E_A}^2}\right), \quad (10)$$

is assumed, the lognormal distribution of the relaxation times emerges in a “natural” way. A comparison with Eq. (4) yields the relations

$$\tau_0 = \tau_\infty \exp\left(\frac{E_0}{k_B T}\right), \quad (11)$$

between the average logarithmic relaxation time and the average activation energy, and

$$\sigma_{\ln \tau} = \frac{\sigma_{E_A}}{k_B T}, \quad (12)$$

between the widths of the distributions of activation energy and relaxation time.²¹ So the average logarithmic relaxation time follows an Arrhenius law and the logarithmic width decreases inverse proportionally to the temperature. The former relation (11) reflects that the average activation en-

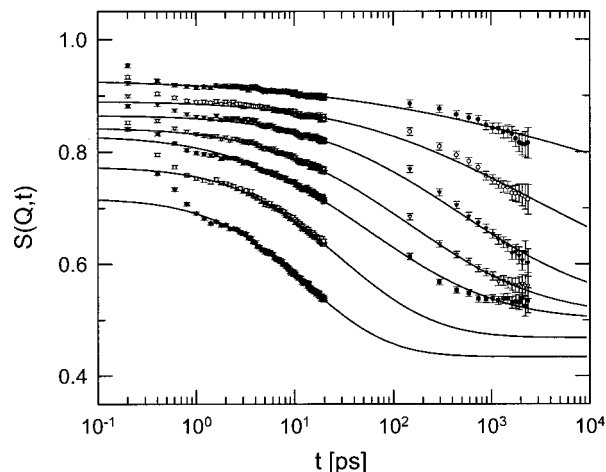


FIG. 6. Intermediate scattering function $S(Q,t)$ (multiple scattering corrected) of PI-d5 at $T=90$ K (filled circles), $T=110$ K (open circles), $T=130$ K (filled triangles), $T=150$ K (open triangles), $T=170$ K (filled squares), $T=200$ K (open squares), and $T=240$ K (filled diamonds) for $Q = 1.57 \text{ \AA}^{-1}$. The lines are fits with the model described in Sec. IV.

ergy does not change with temperature. The latter (12) implies that the attempt frequency τ_∞^{-1} is not distributed. If there were a distribution also in the attempt frequency, Eq. (12) would have to be changed to

$$\sigma_{\ln \tau} = \sqrt{\left(\frac{\sigma_{E_A}}{k_B T}\right)^2 + \sigma_{\ln \tau_\infty}^2}. \quad (13)$$

In order to study the shape of the relaxation function $\phi(t)$ over a large temperature range, the highest accuracy can be obtained by studying Q values with a small EISF. For the IN16 and IN5 experiment this condition is best fulfilled for the highest detector group at $Q = 1.57 \text{ \AA}^{-1}$ (Fig. 6). The fits with Eqs. (3)–(5) were done with the apparent EISF $A_{\text{app}}(1.57 \text{ \AA}^{-1})$ fixed to the value expected for the threefold jump model corrected by Eqs. (7) and (8), namely 0.6047.

It can be seen that the fits represent $S(Q,t)$ well in the range of IN5 data above $t = 1$ ps. The agreement is not so good for the IN16 part. But here it has to be taken into account that due to the ω dependence in the statistical errors of the raw $S(Q,\omega)$ data correlations in the errors of the Fourier transform $S(Q,t)$ can be expected.²² Therefore, the seemingly systematic deviation is not an argument for rejection of the fit as long as the fit lies within the error bounds for 68% of the points.

Figure 7 shows an Arrhenius plot of the average logarithmic relaxation time and the logarithmic width of the distribution, i.e., τ_0 and $\sigma_{\ln \tau}$ of Eq. (5).

The fit of the Arrhenius law, Eq. (11), yields an average activation energy $E_0 = 9.7 \pm 0.4 \text{ kJ/mol} = 1170 \pm 50 \text{ K} \cdot k_B$ and the prefactor $\tau_\infty = 0.10 \pm 0.04 \text{ ps}$. It has to be noted that all temperatures were included in the fit, but because of its large error the value at $T = 90 \text{ K}$ was negligibly weighted. The Arrhenius law represents the τ_0 values in the range 110–240 K well but a small curvature can be noticed. Indeed, fitting alternatively the Vogel–Fulcher^{23,24} expression,

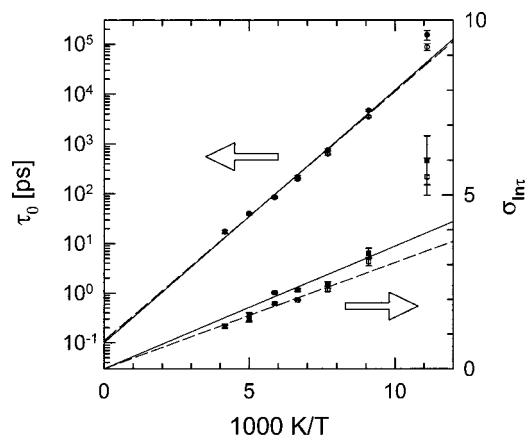


FIG. 7. Circles, left axis: Average logarithmic relaxation times of the methyl group reorientation versus reciprocal temperature. The lines show fits with the Arrhenius law, Eq. (11). Squares, right axis: Logarithmic widths of the distribution of relaxation times. The lines show fits with Eq. (12). For both plots empty symbols represent values obtained without a multiple scattering correction.

$$\tau_0 = \tau_\infty \exp\left(\frac{B}{T - T_0}\right), \quad (14)$$

gives $T_0 = 39 \pm 2$ K, which is much lower than the Vogel–Fulcher temperatures commonly observed but nevertheless significantly different from zero.

Concerning the logarithmic width one can see that the proportionality to $1/k_B T$ is well fulfilled. From the slope $\sigma_{E_A} = 2.93 \pm 0.08$ kJ/mol $= 353 \pm 10$ K $\cdot k_B$ can be calculated. This corresponds to a relative width of 30% for the distribution of activation energies. The fit of the alternative expression (13) with $\sigma_{\ln \tau_\infty}^2$ as a free parameter yields $\sigma_{\ln \tau_\infty}^2 = -0.2 \pm 1.0$, clearly showing that there is no indication of a distribution in the prefactor τ_∞ .

To give an idea about the importance of multiple scattering corrections, values from uncorrected data are also included in Fig. 7. The influence on the average logarithmic relaxation time is obviously small. The Arrhenius parameters are only insignificantly changed: $E_0 = 9.6 \pm 0.3$ kJ/mol $= 1160 \pm 40$ K $\cdot k_B$ and $\tau_\infty = 0.11 \pm 0.03$ ps. This is mainly a consequence of the high Q data used here because these are less affected by multiple scattering. For the distribution width the multiple scattering correction seems to be more important. Although $\sigma_{\ln \tau}$ is still proportional to $1/k_B T$, the widths are smaller and a narrower distribution of activation energies with $\sigma_{E_A} = 2.54 \pm 0.05$ kJ/mol $= 306 \pm 6$ K $\cdot k_B$ would be obtained. The reason for this is that the mismatch between the IN5 and IN16 part in the uncorrected $S(Q, t)$ causes the fit to interpolate with a slightly less “stretched” relaxation function $\phi(t)$.

In order to check the compatibility we have also fitted the elastic scan data from the earlier backscattering experiment⁶ on IN10 in the framework of the current paper (Fig. 8). The resolution function of the instrument was assumed to be a Lorentzian with a full width at half-maximum (FWHM) of 1 μ eV. Taking into account the distribution of relaxation times, the EISF and the DWF, one obtains the theoretically expected height of the elastic peak as

$$S_{\text{el}}(Q) = e^{-\langle u_{\text{fast}}^2 \rangle Q^2/3} \left([1 - A_{\text{app}}(Q)] \times \int \frac{1}{\pi} \frac{1}{h + \tau^{-1}} g(\ln \tau) d \ln \tau + A_{\text{app}}(Q) \right), \quad (15)$$

where $g(\ln \tau)$ is given by Eqs. (9)–(11). For the mean-square displacement of the fast motions a linear dependence on temperature (which is the theoretically expected result for classical harmonic oscillations) $\langle u_{\text{fast}}^2 \rangle = a \cdot T$ was assumed. Finally, there would be five fit parameters: τ_∞ , E_A , σ_{E_A} , a , and an overall intensity factor necessary because $S_{\text{el}}(Q)$ is not known on an absolute scale. It turns out that including the prefactor τ_∞ leads to an instability of the fit. Therefore it was fixed to the value resulting from transition state theory (see below), namely $\tau_\infty = 0.06$ ps. Only the elastic scan at scattering vector $Q = 1.88 \text{ \AA}^{-1}$ was used with the EISF from Eq. (7) at that Q .

The fit results in $E_0 = 1117 \pm 16$ K $\cdot k_B$ close to what is obtained here from the quasielastic spectra. Nevertheless, the width of the energy distribution and $\sigma_{E_A} = 303 \pm 8$ K $\cdot k_B$ is significantly different, but close to the value calculated without a multiple scattering correction. The fit of the proportionality factor yields $a = (10.3 \pm 1.1) \times 10^{-4} \text{ \AA}^2/\text{K}$ that is much higher than the one reported earlier,⁶ $2.9 \times 10^{-4} \text{ \AA}^2/\text{K}$. There are three possible reasons for this discrepancy: (1) The $\langle u_{\text{fast}}^2 \rangle$ here comprises the fast motions of methyl group protons due to overall “phononic” vibrations and the libration of the methyl group. Therefore, it is expected to be higher than the average $\langle u_{\text{fast}}^2 \rangle$. (2) It is also known, e.g., for polybutadiene, which has a similar microstructure but no methyl groups that the experimental mean-square displacement starts to deviate from the harmonic low-temperature extrapolation already near $T = 140$ K. These deviations increase with temperature until near T_g ; a drastic increase of the mean-square displacement is observed. Thus, the validity of an artificial separation into a harmonic DWF that persists even when passing from the glass to the melt and into additional relaxations has to be questioned as well and a higher DWF around $T = 100$ K might be plausible. (3) It may be possible that the temperature range 2–30 K from which a was determined in Ref. 6 may have been too low. It is expected that due to quantum effects the slope of $\langle u_{\text{fast}}^2 \rangle(T)$ reduces close to absolute zero temperature.

Despite this fair agreement, there is still a discrepancy, namely if one calculates the average relaxation times and compares them with those from the quasielastic spectra here. For example, for $T = 110$ K, where the elastic scan shows its point of inflection and thus should give a reliable value, one gets $\tau_0(110 \text{ K}) = 1.5 \pm 0.2$ ns. The corresponding value in Fig. 7 is $\tau_0(110 \text{ K}) = 4.7 \pm 0.2$ ns, three times as much. This may be a consequence of the multiple scattering present in the IN10 elastic scans, where a different sample geometry was used.

V. CONCLUSIONS

Concerning the structural aspect of the methyl group motion our experiments did not give rise to doubts on the validity of the jump model in a threefold potential. After

several corrections a satisfactory agreement of the experimentally obtained elastic incoherent structure factor (EISF) and that from theoretical considerations can be obtained. The absence of one or the other of these corrections in earlier studies may have obscured this.

Nevertheless, the wave vector range $Q \leq 1.57 \text{ \AA}^{-1}$ (neither the larger range up to 1.9 \AA^{-1} accessible by backscattering only) does not allow the distinction of models with an identical length scale l defined as follows: The universal low Q behavior of the EISF is $A(Q) = 1 - Q^2 l^2 / 6 + \mathcal{O}(Q^4)$. A comparison of different models shows that the fourth-order term does not yet play an important role in our Q range. So all we can say is that the results agree with the length scale $l = \sqrt{2}R = 1.45 \text{ \AA}$ predicted by the threefold jump model, but not that this is the only possible model.

In order to distinguish these models, experiments at higher wave vector Q have to be performed, preferably at $Q = 2.59/R = 2.53 \text{ \AA}^{-1}$, where expression (6) shows its characteristic minimum.

The dynamics of the methyl group rotation shows complete agreement with the rotation rate distribution model.^{7,9} Especially, the activation energy distribution (i.e., the “energy landscape”) seems to be unchanged in the investigated temperature range and the attempt frequency (the prefactor in the Arrhenius law) shows no distribution.

In passing, we note that the reduction of the logarithmic width of the relaxation time distribution with temperature, Eq. (12), agrees with the finding from fits with a Kohlrausch function $\phi(t) = \exp[-(t/\tau)^\beta]$ that the stretching exponent β increases with temperature. Indeed, the logarithmic width of the relaxation time distribution corresponding to the Kohlrausch function is²⁵

$$\sigma_{\ln \tau}^{\text{Kohlrausch}} = \frac{\pi}{\sqrt{6}} \sqrt{\frac{1}{\beta^2} - 1}. \quad (16)$$

Inverting this relation, we conclude that the variation of $\sigma_{\ln \tau}$ in our experiment is roughly equivalent (neglecting the fact that the Kohlrausch function corresponds to an asymmetric distribution) to an increase from $\beta(100 \text{ K}) = 0.34$ to $\beta(250 \text{ K}) = 0.67$. This agrees fairly with the experimentally observed change $\beta(100 \text{ K}) = 0.50$ to $\beta(250 \text{ K}) = 0.66$ in another polymer, polymethylmethacrylate.⁸

The prefactor itself, $\tau_\infty = 0.10 \pm 0.04 \text{ ps}$, shows rather good agreement with the value expected from transition state theory (TST): TST predicts the rate of crossing a barrier of height E_A to be

$$r_{\text{TST}} = \frac{\omega_0}{2\pi} \exp\left(-\frac{E_A}{k_B T}\right), \quad (17)$$

where ω_0 is the frequency of the libration in the potential minimum. The latter was determined⁶ as $\hbar\omega_0 = 23.5 \text{ meV}$, yielding $r_{\text{TST}}(T=\infty) = 5.7 \times 10^{12} \text{ s}^{-1}$. Because for the threefold-jump model the relaxation time is related to the rate by $\tau = 1/3r$, one would expect $\tau_\infty = 0.06 \text{ ps}$.

The slightly lower value of the observed rate is also expected from theoretical grounds because models based on the Fokker–Planck equation always give smaller rates than TST.²⁶ But a quantitative use of these models is not possible

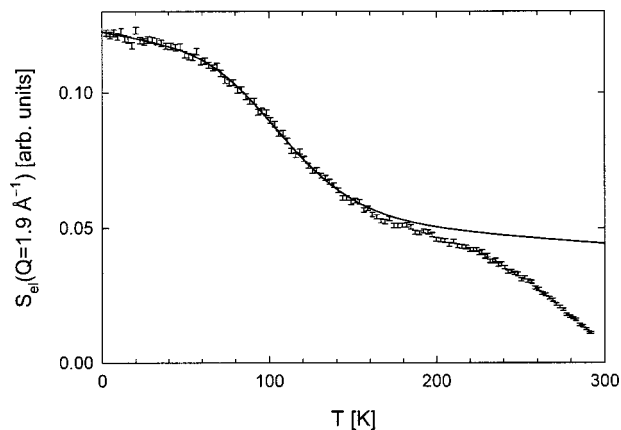


FIG. 8. Elastic scan data of PI-d5 at $Q = 1.88 \text{ \AA}^{-1}$ (error bars). The line is a fit assuming a Lorentzian resolution function of 1 \mu eV FWHM.

here because knowledge of the microscopic friction would be necessary. Nevertheless, the qualitative result of Ref. 26 that the deviation from the TST rate increases at higher temperatures would explain the curvature in the Arrhenius plot, Fig. 7.

We note that two other explanations of this deviation from the Arrhenius law can be ruled out.

- (1) Although some data points stem from temperatures above T_g , the α relaxation characteristic time (e.g., from dielectric spectroscopy:²⁷ 25 \mu s at 240 K) is still many orders of magnitude higher than the relaxation times observed here. So with respect to the methyl group reorientation, the environment is static. Furthermore, the effect should be opposite, i.e., at high temperatures the reorientation should be facilitated.
- (2) Recently, the importance of tunneling for the methyl group dynamics at low temperatures has been demonstrated.^{4,28} This quantum effect leads to additional inelastic intensity in the spectra containing a broad distribution of tunneling lines. If such spectra were treated in the way done here, this intensity would be misinterpreted as additional quasiclastic broadening. Therefore, the effect should be an opposite deviation from the Arrhenius law toward smaller apparent relaxation times at low temperatures.

Some doubt may be possible concerning the shape of the activation energy distribution. The discrepancies of the fits to $S(Q, t)$, especially in the long time range of IN16, may indicate that a skewed distribution has to be used. But we consider the present data not to be sufficiently precise to define an additional fit parameter besides the center and the width of the distribution.

Finally, we have shown the significance of multiple scattering corrections in two points: (1) Without multiple scattering correction the EISF does not show the *a priori* required low Q behavior and therefore cannot be represented by any model. (2) The shape of the relaxation function $\phi(t)$ obtained from the experiment is significantly affected by the absence of multiple scattering corrections. Interestingly, the effect on the average logarithmic relaxation time is much

smaller, at least if only the highest Q data is used for its determination.

ACKNOWLEDGMENTS

The authors thank M. Holschbach for supplying the NMR data revealing the incomplete deuteration of the sample.

APPENDIX: MULTIPLE SCATTERING CORRECTION

The multiple scattering method used here²⁹ is a purely analytical method and does not rely on complicated numerical procedures such as Monte Carlo simulation. It uses only experimental data and one parameter describing the multiple scattering magnitude. No prior knowledge of the spectral shape of $S(Q, \omega)$ is necessary, as in the case of Monte Carlo algorithms. It differs from those procedures that are currently in use mainly in that it operates on the intermediate scattering function $S(Q, t)$ obtained by an inverse Fourier transform as described in the preceding section and not the scattering function $S(Q, \omega)$ itself. It turns out that this mode of operation indeed facilitates the calculations if the following approximations are used.

- (1) The fraction of neutrons scattered $n+1$ times with respect to those scattered n times is independent of n .
- (2) Neutrons that are scattered at least twice coherently are distributed isotropically.

Adopting these approximations the apparent scattering function $\hat{S}(Q, \omega)$ can be expressed as a series of terms from neutrons scattered n times:

$$\hat{S}(Q, \omega) = S(Q, \omega) + s \cdot \bar{S}(\omega) \otimes \bar{S}(\omega) + s^2 \cdot \bar{S}(\omega) \otimes \bar{S}(\omega) \otimes \bar{S}(\omega) + \dots \quad (\text{A1})$$

Here $\bar{S}(\omega)$ denotes the solid-angle average of the “true scattering function $S(Q, \omega)$ ”, \otimes the convolution in ω , and s the ratio between $n+1$ th and n th scattering intensity.

An inverse Fourier transform of (A1) changes the self-convolutions into powers:

$$\hat{S}(Q, t) = S(Q, t) + s \cdot \bar{S}(t)^2 + s^2 \cdot \bar{S}(t)^3 + \dots, \quad (\text{A2})$$

resulting in a geometric series³⁰ that can be summed up to

$$\hat{S}(Q, t) = S(Q, t) + \frac{s \cdot \bar{S}(t)^2}{1 - s \cdot \bar{S}(t)}. \quad (\text{A3})$$

This equation can be solved for the multiple scattering corrected scattering function:

$$S(Q, t) = \hat{S}(Q, t) - \frac{s \cdot \bar{S}(t)^2}{1 + s \cdot \bar{S}(t)}, \quad (\text{A4})$$

where $\bar{S}(t)$ denotes the solid-angle average of the apparent scattering function.

With respect to the multiple scattering parameter s a cautionary remark is in order: In principle, it is possible to calculate this parameter from the sample geometry and scattering cross section by numerical or (for simple geometries) analytical means. In practice, one has to face two difficulties

in such an attempt: (1) Especially for thin samples the shape is difficult to control exactly and this necessary input to the calculation is not available. (2) It can be seen from Eq. (A4) that if $S(Q, t)$ is scaled by a factor f , s has to be rescaled by $1/f$ to obtain the same multiple scattering effect. This means that the procedure is not invariant to a normalization error of $S(Q, t)$, which often happens in the experiment due to uncontrolled sample or (vanadium) normalization sample amounts.

Therefore, it is often necessary to use *a posteriori* criteria that determine s by “plausibility checks” on $S(Q, t)$. If sufficiently low Q detectors are available, such a criterium may be that inelastic scattering has to vanish in the low Q limit, i.e., in the time domain $S(Q \rightarrow 0, t) \equiv \text{const.}$

Another caveat to be observed is that in experiments as those described here that aim at the measurement of the incoherent scattering function, a non-negligible amount of coherent scattering has to be taken into account. Because only few instruments (using polarized neutrons) can discriminate coherent and incoherent scattering in practice the normalized intermediate scattering function,

$$S_n(Q, t) = S(Q, t)/S(Q), \quad (\text{A5})$$

is used in lieu of the incoherent intermediate scattering function. In other words, Eq. (A5) forces the natural limit $S_{\text{inc}}(Q, t \rightarrow 0) = 1$ of the incoherent intermediate scattering function upon a mixture of incoherent and coherent scattering.

This step is often combined with the division of the Fourier transformed data by the Fourier transformed resolution. If one uses the sample at low temperature for the resolution determination by a measurement of the sample at low temperature in (2) the “deconvolution” and the normalization (A5) can be done at the same time provided $S(Q)$ does not change too much with temperature (which is the case for polymeric glass formers²⁰).

The situation is more complicated if the multiple scattering correction described here is used; the two steps of “deconvolution” of t dependence and “normalization” of Q dependence have to be done separately. The change of the total scattered intensity by the normalization (A5) would not leave (A4) invariant. Therefore, at first a normalized resolution function has to be calculated from the low-temperature measurement by dividing the low-temperature spectrum $\hat{S}_0(Q, \omega)$ by its integral $\hat{S}(Q)$. This normalized resolution when used in (2) does not change the Q dependence of the intensity, but only removes the resolution effect. Then $\hat{S}(Q, t)$ and $\hat{S}(Q)$ have to be multiple scattering corrected by (A4) and its analog with the t dependence omitted, respectively. Finally, the multiple scattering corrected functions have to be combined by (A5) to obtain the normalized intermediate scattering function.

¹N. G. McCrum, B. E. Read, and G. Williams, *Anelastic and Dielectric Effects in Polymer Solids* (Wiley, New York, 1967).

²C. A. Angell, *Science* **267**, 1924 (1995).

³F. Alvarez, A. Alegría, J. Colmenero, T. M. Nicholson, and G. R. Davies, *AIP Conf. Proc.* **479**, 201 (1999).

⁴J. Colmenero, R. Mukhopadhyay, A. Alegría, and B. Frick, *Phys. Rev. Lett.* **80**, 2350 (1998).

- ⁵B. Gabrys, J. S. Higgins, K. T. Ma, and J. E. Roots, *Macromolecules* **17**, 560 (1984).
- ⁶B. Frick and L. J. Fetters, *Macromolecules* **27**, 974 (1994).
- ⁷A. Chahid, A. Alegría, and J. Colmenero, *Macromolecules* **27**, 3282 (1994).
- ⁸V. Arrighi, J. S. Higgins, A. N. Burgess, and W. S. Howells, *Macromolecules* **28**, 2745 (1995).
- ⁹R. Mukhopadhyay, A. Alegría, J. Colmenero, and B. Frick, *Macromolecules* **31**, 3985 (1998).
- ¹⁰J. T. Gotro and W. Graessley, *Macromolecules* **17**, 2767 (1984).
- ¹¹R. Zorn, G. B. McKenna, L. Willner, and D. Richter, *Macromolecules* **28**, 8552 (1995).
- ¹²D. Richter, B. Frick, and B. Farago, *Phys. Rev. Lett.* **61**, 2465 (1988).
- ¹³See, e.g., W. Knaak, F. Mezei, and B. Farago, *Europhys. Lett.* **7**, 529 (1988); W. Petry, E. Bartsch, F. Fujara, M. Kiebel, H. Sillescu, and B. Farago, *Z. Phys. B: Condens. Matter* **83**, 175 (1991); J. Colmenero, A. Arbe, and A. Alegría, *Phys. Rev. Lett.* **71**, 2603 (1993); J. Wuttke, W. Petry, G. Coddens, and F. Fujara, *Phys. Rev. E* **52**, 4026 (1995); and Ref. 8.
- ¹⁴R. Zorn, A. Arbe, J. Colmenero, B. Frick, D. Richter, and U. Buchenau, *Phys. Rev. E* **52**, 781 (1995).
- ¹⁵B. Gabrys and O. Schärpf, *Physica B* **180&181**, 495 (1992).
- ¹⁶Because polarization analysis is only able to distinguish *spin-incoherent* neutron scattering and not that due to isotopic incoherence, the σ_{inc} values in Eq. (8) must only include the former part of the incoherent cross section.
- ¹⁷R. Zorn, D. Richter, J. Eilhard, A. Zirkel, L. J. Fetters, F. Alvarez, and J. Colmenero, *IFF Scientific Report*, Forschungszentrum Jülich, Jülich, Germany, 2001, p. 119.
- ¹⁸R. Zorn, *Nucl. Instrum. Methods, Phys. Res. A* (in press).
- ¹⁹P. Wells and R. Cywinski, *Aust. J. Phys.* **34**, 193 (1981); J. Mayers and R. Cywinski, *Nucl. Instrum. Methods Phys. Res. A* **241**, 519 (1985).
- ²⁰B. Frick, D. Richter, and Cl. Ritter, *Europhys. Lett.* **9**, 557 (1989).
- ²¹These two relations can be derived more generally by calculation of the (logarithmic) moments from Eq. (9) without assuming a specific distribution of activation energies.
- ²²Equation (1) shows that every measured data point $S(Q, \omega_i)$ influences a certain calculated $S(Q, t_i)$ value to the same absolute amount. Therefore, the errors of $S(Q, t_i)$ are, in general, correlated even if the $\Delta S(Q, \omega_i)$ are not. A calculation of the error propagation shows that the $\Delta S(Q, t_i)$ are uncorrelated if and only if $\Delta S(Q, \omega_i) \equiv \text{const.}$ Because for scattering methods the statistical error is $\Delta S(Q, \omega_i) \propto \sqrt{S(Q, \omega_i)}$, and there is a large quasielastic peak in $S(Q, \omega)$ this condition is clearly not fulfilled here.
- ²³H. Vogel, *Phys. Z.* **22**, 645 (1921).
- ²⁴G. S. Fulcher, *J. Am. Ceram. Soc.* **8**, 339 (1925).
- ²⁵R. Zorn (unpublished).
- ²⁶B. Carmeli and A. Nitzan, *Phys. Rev. Lett.* **51**, 233 (1983).
- ²⁷D. Boese and F. Kremer, *Macromolecules* **23**, 829 (1990).
- ²⁸A. J. Moreno, A. Alegría, and J. Colmenero, *Phys. Rev. B* **59**, 5983 (1999).
- ²⁹C. Pecharrmán (personal communication, 1995).
- ³⁰The procedure here is formally analogous to the multiple scattering correction devised for elastic scattering of polarized neutrons in Ref. 19.